Two-dimensional spatially ordered arrays of cobalt nanowires: polarized SANS study

2010 J. Phys.: Conf. Ser. 247 012033

(http://iopscience.iop.org/1742-6596/247/1/012033)

Journal of Physics: Conference Series **247** (2010) 012033 doi:10.1088/1742-6596/247/1/012033

Two - dimensional spatially ordered arrays of cobalt nanowires: polarized SANS study

A.P. Chumakov[1], S.V. Grigoriev [1], N.A. Grigoryeva[2], K.S. Napolskii[3], I.V. Roslyakov[3], A.A. Eliseev[3], A.I. Okorokov [1], H. Eckerlebe[4]

[1]Petersburg Nuclear Physics Institute, Gatchina, 188300 St.Petersburg, Russia

[2]Faculty of Physics, St-Petersburg State University, 198504 St-Petersburg, Russia

[3]Department of Materials Science, Moscow State University, 119992 Moscow, Russia

[4]GKSS Forschungszentrum, 21502 Geesthacht, Germany

E-mail: chumakov@lns.pnpi.spb.ru

Abstract. Structural and magnetic properties of two-dimensional spatially ordered system of ferromagnetic cobalt nanowires embedded into Al_2O_3 matrix have been studied using polarized small-angle neutron scattering. The small-angle scattering pattern exhibits many diffraction peaks (up to the third reflection order), which corresponds to the scattering from highly correlated hexagonal structure of pores and magnetic nanowires. A comprehensive analysis of contributions to the scattering intensity, including nonmagnetic (nuclear) contribution, magnetic contribution depending on the magnetic field, and nuclear-magnetic interference indicating the correlation between the magnetic and nuclear structures was carried out. A detailed pattern of the remagnetization of an ordered array of the magnetic nanowires has been obtained. It has been illustrated that polarized neutron scattering provides unique information inaccessible by the standard magnetometry techniques.

1. Introduction

One of the most important challenges in physics and materials science today is the preparation of ordered nanostructure arrays with the controlled properties and dimensions. Anodic aluminium oxide (AAO) films formed by two-step anodization technique [1] or nanoimprint technology [2] are well-known to possess uniform pore structure with hexagonal arrangement of cylindrical channels, which makes them an extremely attractive matrix or reactor for synthesis of nanowires. The unique microstructure of AAO templates opens a pathway for growing ordered arrays of nanowires with ultimately high length at very low diameters (which could be considered as one-dimensional) [3]. These composites could be used as a perfect model objects for deeper understanding of magnetization reversal processes in spatially-ordered systems on nanolevel.

A number of works report controllable growth and investigation of magnetic nanowires, however most of them involve only magnetometry studies, which are known to provide integral characteristic of bulky system and give no information on organization of magnetic material [4]. The small-angle polarized-neutron scattering method is much more rarely used, although this technique is sensitive both to organization [5] and the magnetic properties of the nanostructured media [6,7].

The present study is focused on the SANS investigation of the spatially ordered arrays of Co nanowires grown in AAO templates.

2. Synthesis and Experimental Details

Preparation of spatially ordered arrays of cobalt nanowires was carried out by metal electrocrystallization inside the channels of anodic alumina films with a thickness of 110 μm. In order to obtain better ordering of the channels, the anodic aluminium oxide membranes were prepared by the two-step anodization technique [1, 2, 8]. The anode oxidation of aluminium is performed in a two-electrode electrochemical cell in a 0.3 M $(COOH)_2$ solution at a DC voltage of 40 V for 50 and 42,5 h in the first and second anodization stages, respectively. The procedure of fabrication of electrodes on AAO films is described in details elsewhere [7, 9].

Electrodeposition of cobalt was carried out in three-electrode cell from 0.3M $CoSO_4$ + 0.05M $CoCl_2$ + 0.3M H_3BO_3 solution at deposition potential E_d = -0.8 V versus Ag/AgCl reference electrode using Autolab PGSTAT 302 potentiostat. The Pt wire serves as a counter electrode. The duration of the Co electrodeposition was 1.5 h, which corresponds, according to scanning electron microscopy, to the formation of nanowires with a length of 34.5 μm and a diameter of about 40 nm. Figure 1 presents the SEM pictures of a side view of the AAO film with arrayed Co nanowires on a bottom part (a) and a view of the Co wires obtained after solution of the alumina membrane (b).

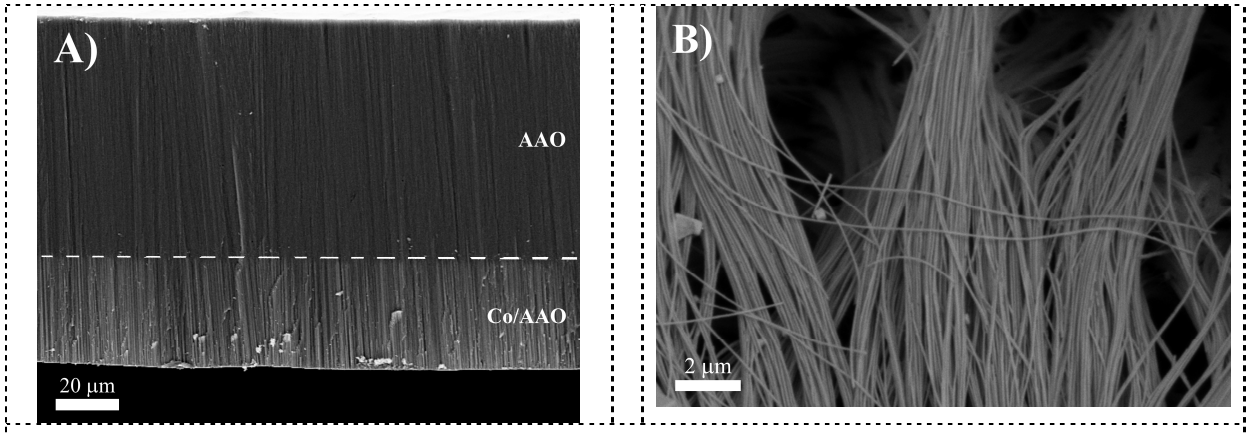

Figure 1. The SEM data: a side view of the anodic alumina film with arrayed Co nanowires (a) and a view of the Co wires after solution of the alumina membrane (b).

Polarized SANS measurements were carried out at the SANS-2 beamline of Geesthacht Neutron Facility (GeNF). Polarized neutron beam with mean wavelength of $\lambda = 0.7$ nm, wavelength spread of $\Delta\lambda/\lambda = 10\%$ and initial polarization $P_0 = 0.95$ was used at. A film with an area of 0.3 cm^2 was oriented perpendicularly to the neutron beam and was uniformly irradiated over the entire area. Such an orientation of the sample corresponds to parallel orientation of the pores and the long axis of the magnetic nanowires to the incident neutron beam. The chosen geometry of the experiment allows the observation of diffraction reflections from the ordered system of pores or magnetic wires in a small-angle scattering range. The sample-to-detector distance of 14 m was used with appropriate collimations to cover scattering vectors Q from 0.025 to 0.17 nm^{-1}. An external magnetic field (up to 800 mT) was applied in the horizontal plane perpendicular to the incident beam (and perpendicular to the long axis of the nanowires). We determine the total (nuclear and magnetic) scattering ($I(Q) = I^+(Q) + I^-(Q)$) and the polarization dependent part of the scattering ($\Delta I(Q) = I^+(Q) - I^-(Q)$), where $I^+(Q)$ and $I^-(Q)$ are the intensities for neutrons polarized parallel (+) and anti-parallel (–) to the magnetic field. The field-dependent scattering intensity is extracted as $I_H(Q) = I(Q,H) - I(Q,0)$. The polarized SANS data were taken at room temperature.

3. Results

A magnetization curve with the magnetic field in the plane of the sample and perpendicular to the nanowires, that corresponds to the polarized SANS experiment, were recorded using SQUID magnetometer Cryogenics S-700 at the temperature 290 K. Figure 2 present the magnetization curve saturated above H = 800 mT. A small hysteresis loop is observed in the range from -300 mT to 300 mT. There is hardly noticeable change in a slope of the magnetization curve in the range of small field within ± 100 mT as compare to the range of larger fields from 100 mT to 300 mT. This feature may be related to the change in a mechanism of the sample's magnetization.

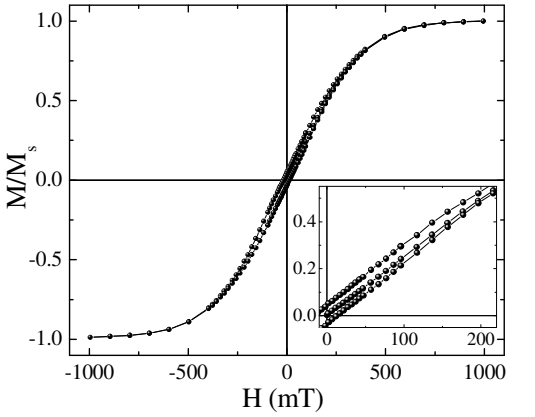

Figure 2. Magnetization curve for Co nanowires embedded into alumina membrane in the field applied perpendicular to the long axis of the wires.

A typical neutron diffraction pattern measured from Co nanowire array grown inside AAO membrane is shown in Figure 3 a. The first and the second order reflections have been detected, suggesting the presence of strong correlations in the positions of the pores (or nanowires) over significant distances. The hexagonally arranged set of reflections demonstrates the 6-fold symmetry of the structure. For the considered geometry the interplanar spacing d_{hk} can be calculated as $d_{hk} = \sqrt{3}a/(2\sqrt{h^2 + hk + k^2})$., where a – is a unit cell parameter of 2D superlattice.

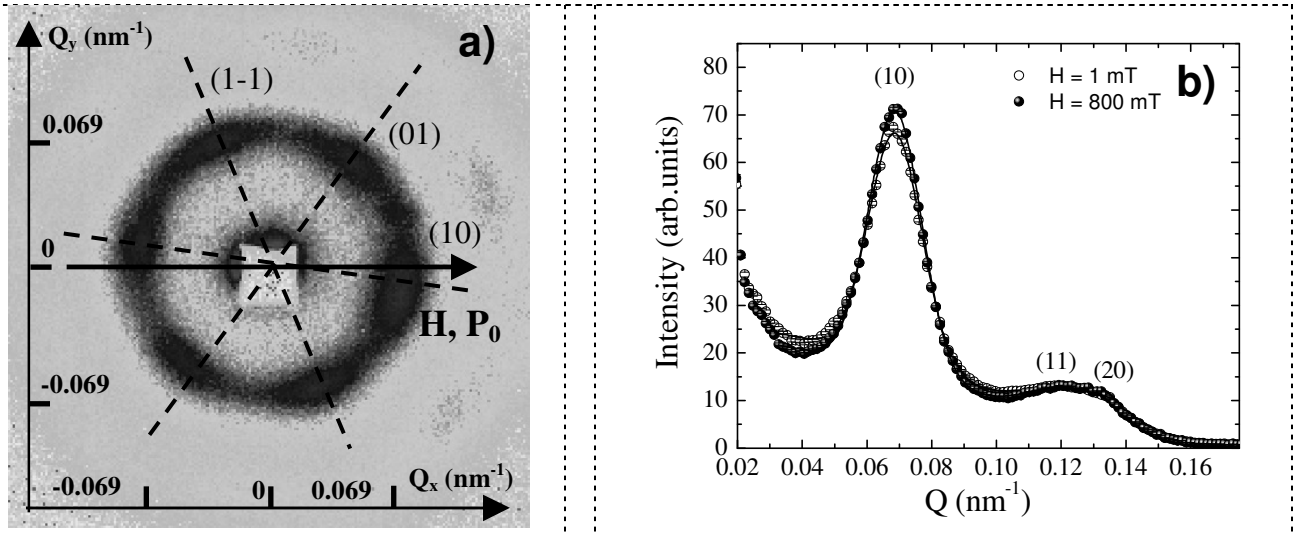

Figure 3. Typical 2D neutron diffraction pattern from Co/Al_2O_3 nanocomposite with spatially ordered

structure (a). Momentum-transfer dependence of the total (nuclear and magnetic) neutron scattering intensity at H = 1 and 800 mT (b).

The widening of reflections to 10-20 degrees in an azimuthal direction, shown in Figure 3 a, indicates that samples have a block structure, with slight disorientation of domains in the plane of the film. Nevertheless, the diffraction patterns, typical for a quasi-single crystal, were recorded using a neutron beam of 5 mm diameter, suggesting correlated orientation of the domains on the irradiated area (~ 0.3 cm^2). Similar results had been observed previously for pure anodic aluminium oxide membranes by SANS techniques [5].

Figure 3 b illustrates the momentum-transfer dependence of the total (nuclear and magnetic) neutron scattering $I(Q)$ for the nonmagnetized (H = 1 mT) and magnetized (H = 800 mT) sample. Several diffraction maxima are clearly observed, indicating the highly ordered structure of the Co/Al_2O_3 nanocomposite. The momentum transfer dependence $I(Q)$ is satisfactorily reproduced by the sum of the Gaussian components with the centers located at $Q_{10} = 0.069 \pm 0.004$ nm^{-1}, $Q_{11} = 0.119 \pm 0.004$ nm^{-1}, $Q_{20} = 0.138 \pm 0.004$ nm^{-1}, and fixed half-width of $w = 0.0090 \pm 0.0005$ nm^{-1}; coupled with a diffuse small-angle scattering, represented by an exponential decay. The observed diffraction maxima are classified in the hexagonal lattice with the parameter $a = 106 \pm 2$ nm. It should be noted that applying the external magnetic field induces noticeable increase of the diffraction peak intensity in the order of 5 % (see Fig. 3 b).

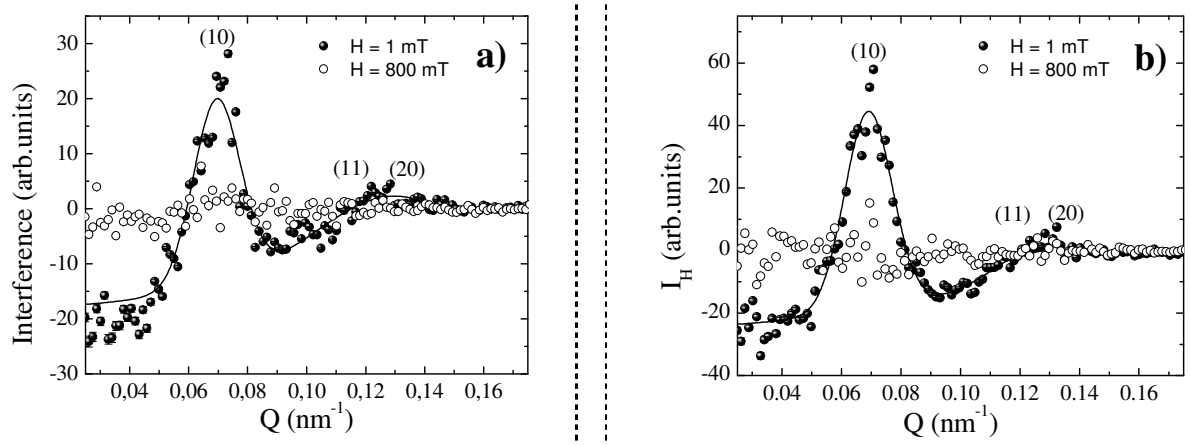

Figure 4. Q-dependence of the nuclear–magnetic interference $\Delta I(Q)$ at H = 1 and 800 mT (a) and magnetic contribution to the scattering $I_H(Q)$ (b).

Figure 4 shows the nuclear-magnetic interference $\Delta I(Q)$ and the field-dependent part of neutron scattering $I_H(Q)$ as a function of scattering vector. The peak positions for the magnetic contributions match the positions of nuclear peaks (at zero magnetic field in Figure 3 b). This confirms the formation of the spatially-ordered magnetic structure, e.g. the ordered array of nanowires with periodicity of 106 nm.

As seen from Figure 4 a, the interference contribution $\Delta I(Q)$ is equal to zero in the entire momentum-transfer range for the unmagnetized sample (H = 1 mT). In high magnetic fields, the polarization-dependent scattering consists of two contributions: interference maxima at Q values coinciding with the positions of diffraction reflections in scattering on the ordered structure of nanowires and interference in diffuse small-angle scattering. These two contributions have opposite signs in a good agreement with theory [6]. The interference scattering can be approximated by the sum of the Gaussians with the centers at zero (diffuse scattering) and at $Q = Q_{hk}$ (coherent scattering). The magnetic field dependence of the interference contribution integrated over the azimuthal angle at $|Q_{10}|$

is shown in Fig. 5 a. Note that the interference contribution is proportional to the magnetization, which exhibits no hysteresis within error bars in initial magnetization or in subsequent remagnetization of the system of magnetic nanowires in the field perpendicular to the long axis of wires. It is interesting to note that the increase of intensity is not gradual but has a bump at H = 150 mT and a deep at H = 200 mT.

The magnetic-field-dependent scattering component $I_H(Q)$ shown in Figure 4 b represents the difference between the magnetic cross sections of the sample in two significantly different states, a state close to saturation magnetization (in a field of H = 800 mT) and a completely demagnetized state. The main component of the magnetic cross section at H = 800 mT is the system of the magnetic reflections described by the sum of Gaussians whose positions correspond to the maxima of the nuclear scattering cross section. On the contrary, the main component of the cross section in zero magnetic field is scattering on domains; i.e., diffuse scattering, which is described by a Gaussian at Q = 0 with no contribution to diffraction reflections. The approximation of the experimental data in the frame of this model is shown in Fig. 4 b. The magnetic field dependence of the most intense magnetic reflection integrated over the azimuthal angle at $Q = |Q_{10}|$ is shown in Fig. 5 b. Firstly, the intensity of the magnetic reflection does not change within error bars with the magnetic field in the range from 0 up to 200 mT. Secondly, the increase of intensity with the field starts at H = 200 mT. Thirdly, the remagnetization process proceeds with hysteresis in the field range above 200 mT.

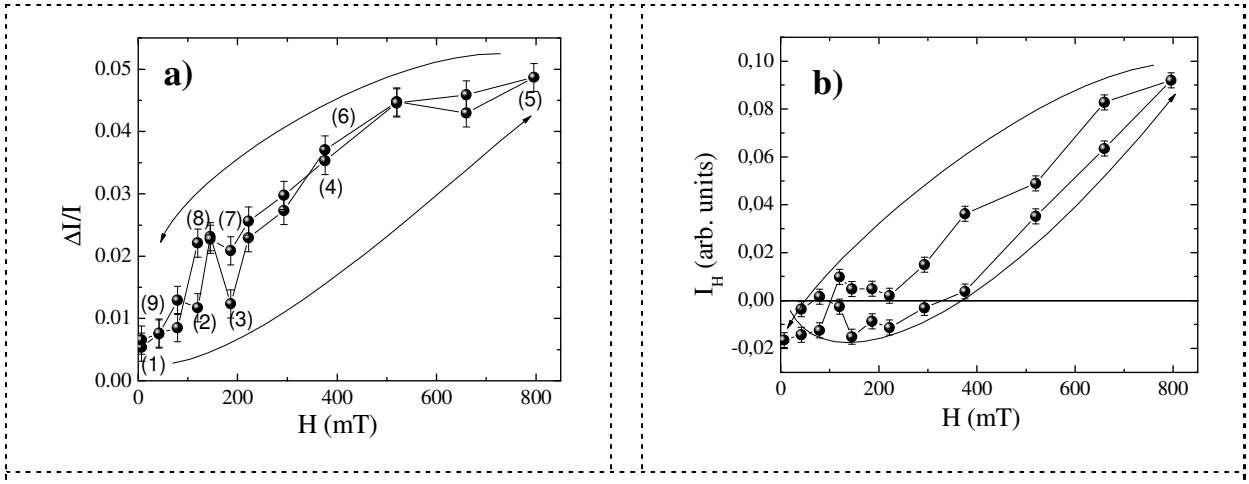

Figure 5. Magnetic field dependence (a) of the interference contribution and (b) the magnetic coherent contribution obtained from the approximation of the experimental data.

The additional features of the intensity of the neutron scattering upon remagnetization in the range of ± 200 mT are well seen in Fig.5. They correspond to the slight change in the slope of the magnetization curve that can be distinguished in Fig.2. The model describing the remagnetization process of the magnetic nanowires array in the perpendicular field is presented in Fig 6. At zero field every nanowire is divided on domains with randomly oriented magnetization, position (1). The orientation of the magnetic moments depends probably on magnetic easy direction of nanowire and the anisotropy and the size of magnetic crystalline particles constituting nanowires. We suppose that domain walls can be bounded to the boundary between crystallites within a nanowire. There is also no reason to believe in correlation between the magnetization in neighboring wires and as a result we expect no interference or pure magnetic contributions to the neutron reflections. When the perpendicular external magnetic field is applied then an orientation of the magnetic moments changes toward the field axis, position (2). The domain walls can be removed in some of nanowires, so that they become single-domain particles. The component of the magnetization along the field axis appears what is reflected in appearance of the nuclear magnetic interference. Further increase in quantity of such single domain nanowires, so that now every wire is a single magnetic domain, position (3),

results in additional dipole interaction between nanowires favoring up-to-down orientations of the magnetic moments in the neighboring wires. This additional dipole interaction competes with the magnetic field and this competition leads to the state where different wires are not correlated. This situation is reflectes in an additional minimum in nuclear-magnetic interference and in pure magnetic contributions to the reflexes. Further increase of the magnetic field starts reorient magnetic moments in directions toward its axis, position (4). The fully saturated magnetization in the nanowires is reached at large magnetic fields, position (5). The subsequent decrease of the magnetic field is shown in positions (6) – (9). The magnetic moments inside the nanowires are differently oriented in positions (6 and 7) as compared to positions (4 and 3), respectively. This configurations of magnetic moments result in hysteresis of magnetic intensity shown in Figure 6 and absence of any hysteresis in the nuclear magnetic interference shown in Figure 5 a. The single-domain nanowires become multidomain again at H = 200 mT, when the dipole interaction competes with the field, position (8). The system becomes fully disordered massive of multidomain nanowires at H = 0, position (9). It should be noted that the described model is a suggestion only and has not been tested by rigorous modeling of the experimental data.

The similar magnetization process was observed in the massive of nickel nanowires [6] but the field range where a disordered state occurs, is limited by H = 100 mT. This difference can be related to the difference in values of the magnetic moments of Co and Ni. It may also well be that crystalline structures of nanowires defined by the crystallization process during synthesis are different for cobalt and nickel.

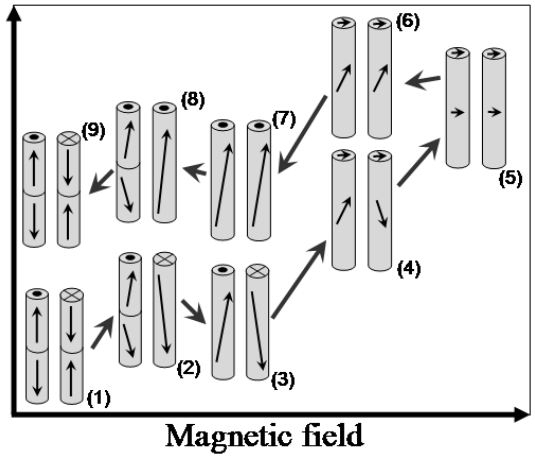

Figure 6. The scheme of the remagnetization model for in magnetic nanowires array. Arrows show the direction of the magnetization while the length of the arrow corresponds rather to the area with homogeneous magnetization but not to the magnetization value.

4. Concluding remarks

In conclusion, we have investigated the process of the remagnetization of the massive of Co nanowires in the magnetic field applied perpendicularly to the long wire's axis. The measurements reveal the presence of hysteresis in field dependence of the magnetic scattering, connected to several processes well reflected in the intensity of the pure magnetic and nuclear-magnetic contributions upon remagnetization. In the ground state (at no field applied) the moments of nanowires are aligned parallel to the long axis, but are randomly distributed between +1 and –1 states and probably in multi-domain state. The magnetic field applied results in a deviation of the average magnetic moment of a wire from its long axes, however, shape and/or crystalline anisotropy, dipole interaction compete with the magnetic field so that the magnetization starts at H larger than 250 mT. Further increase of the field aligns moments in perpendicular direction shown in the rapid increase of scattering intensity of the magnetic reflexes. Thus, the inflection of experimental curve at the $H \approx 250$ mT should be attributed to the change of the magnetization mechanism in the Co nanowires array from incoherent to the coherent rotation. We have represented the model for magnetic moment behavior in cobalt

nanowires embedded into anodic alumina matrix. One can also conclude that polarized-neutron scattering provides information inaccessible to the standard magnetometric methods.

Acknowledgments
This work was performed within the framework of a Federal Agency of Science and Innovations (projects 02.513.11.3485). The Russian authors thank RFBR for partial support (Grant № 10-02-00634). This work was supported by the Presidium of the Russian Academy of Sciences under the Program for Basic Research. The Russian authors are grateful to the GKSS Research Centre (Germany) for hospitality.

References

[1] H. Masuda and K. Fukuda, 1995 Science **268**, 1466.
[2] S. Shingubara, J. Nanopart. 2003 Res. **5**, 17.
[3] G. Sauer, G. Brehm, S. Schneider, et al., 2002 J. Appl. Phys. **2**, 3243.
[4] Y. Piao, H. Lim, J. Y. Chang, et al., 2005 Electrochim. Acta **50**, 2997.
[5] S. V. Grigoriev, N. A. Grigorieva, A. V. Syromyatnikov, et al., 2007 Pis'ma Zh. Éksp. Teor. Fiz. **85**, 549 [2007 JETP Lett. **85**, 449].
[6] S.V. Grigoriev, N.A. Grigorieva, A.V. Syromyatnikov, et al., 2007 Pis'ma Zh. Éksp. Teor. Fiz. **85**, 738 [2007 JETP Lett. **85**, 605].
[7] K.S. Napolskii, A.P. Chumakov, S.V. Grigoriev, N.A. Grigoryeva, H. Eckerlebe, A.A. Eliseev, A.V. Lukashin, Yu.D. Tretyakov. // Physica B, 2009, v. **404**, pp. 2568–2571.
[8] O. Jessensky, F. Muller, and U. Gusele, 1998 Appl. Phys. Lett. **72**, 1173.
[9] K.S. Napolskii, P.J. Barczuk, S.Yu. Vassiliev, A.G. Veresov, G.A. Tsirlina and P.J. Kulesza. // Electrochimica Acta, 2007, v. **52**, pp. 7910–7919.